The influence of cutting conditions on surface integrity of a wrought magnesium alloy

N. Wojtowicz, I. Danis, Frederic Monies, Pascal Lamesle, Rémy Chieragatti

Available online at www.sciencedirect.com

ScienceDirect

Procedia Engineering 63 (2013) 20 – 28

Procedia Engineering

www.elsevier.com/locate/procedia

The Manufacturing Engineering Society International Conference, MESIC 2013

The influence of cutting conditions on surface integrity of a wrought magnesium alloy

N. Wojtowicz[a,*], I. Danis[b], F. Monies[b], P. Lamesle[c], R. Chieragati[a]

[a]*Université de Toulouse, ISAE, Institut Clément Ader, 10 Avenue E. Belin, BP 54032, 31055 Toulouse, France*
[b]*Université de Toulouse, UPS, Institut Clément Ader, 118 Route de Narbonne, 31062 Toulouse cedex, France*
[c]*Université de Toulouse, EMAC, Institut Clément Ader, Campus Jarlard, 81013 Albi cedex 9, France*

Abstract

Surface integrity of machined components has a significant impact on their functional performance. Modification of surface integrity, which includes roughness, residual stress and microstructure may limit product performance such as fatigue life. In this study, the influence of machining conditions in turning on surface integrity of a wrought Mg-Zn-Zr-RE alloy was investigated. First, turned surfaces were obtained through a design of experiments, where input parameters are cutting speed, feed, depth of cut and nose radius. Second, modifications of surface integrity such as tensile/compressive residual stress, microhardness, twinning and surface roughness were correlated with cutting parameters. This study suggests optimal cutting conditions to achieve a given surface integrity and improve fatigue life.

Keywords: Turning; surface integrity; magnesium alloy

1. Introduction

New magnesium alloys with rare earth (RE) elements are increasingly used in aerospace because of their low density, high strength even at high temperatures and good machining capability (Advesian and Baker 2000). Besides, wrought magnesium alloys present higher mechanical properties and corrosion resistance without

* Corresponding author. Tel.: +33-0561-339-154; fax: +33-0561-339-095.
E-mail address: nathalie.wojtowicz@isae.fr

doi:10.1016/j.proeng.2013.08.212

microstructural defects such as porosities unlike casting alloys, which enables aerospace suppliers not to thicken areas in components subjected to mechanical stress and take full advantage of these light weight materials. However, wrought magnesium workpieces require machining, which induce thermo mechanical treatment on surface, which modify microstructure, residual stress and roughness. It has long been recognized that surface integrity factors play a great role in mechanical performance of machined components, such as fatigue life. Sasahara (2005) demonstrated that it is possible to improve fatigue life compared to the virgin material by choosing machining conditions inducing compressive residual stress and high hardness into subsurface. In magnesium alloy, it has been shown that residual stress induced by shot peening have a beneficial effect on fatigue life (Bhuiyan et al 2012, Zhang et al 2010, Liu et al 2013), if surface defects are low. Thus, a comprehensive understanding of cutting parameters effects on surface integrity is essential to determine optimal cutting conditions in Mg-RE alloy. Some authors have studied the influence of coating and lubrication on built-up-edge formation, temperature and cutting forces during machining magnesium alloy (Tonshoff and Winkler 1997, Gariboldi 2003, Bhowmick et al 2010, Fang et al 2005). Denkena et al (2011) investigated the influence of cutting conditions and tool geometry on surface integrity in MgCa0.8 alloy for biomedical application in turning and milling. Effect of edge radius and lubrication (dry or cryogenic) in orthogonal cutting of AZ31B was studied by Pu et al (2012). A white layer of nanograin structure was obtained under cryogenic machining which may improve corrosion resistance. According to authors' knowledge, no work has been done on the influence of dry machining conditions on surface integrity of Mg-RE alloy. In this study, the influence of several cutting parameters on surface integrity in a wrought magnesium alloy is investigated, in order to determine optimal cutting conditions, which may improve fatigue life.

2. Experimental procedure

The forged commercial alloy Elektron21 was used in this study. The material was received in plate of dimensions 60 mm x 320 mm x 300 mm. The chemical composition of the alloy is provided in Table 1. All specimens for machining (20mm x 20 mm x 150 mm) were cut parallel to the long transverse direction and then turned with the same cutting conditions (V_c = 800 rev/min, a_p = 2mm, f = 0.150mm/rev).

Table 1. Chemical composition of Elektron21 (wt.%)

Nd	Gd	Zn	Zr	Mg
2.6-3.1	1.0-1.7	0.2-0.5	Saturated	Balance

2.1. Machining experiments

In order to study the influence of machining conditions on surface integrity a design of experiments (DoE) was set up. Four cutting parameters were considered to be the input parameters of the DoE: cutting speed V_c, feed f, depth of cut a_p and nose radius r_ε, whereas roughness, microstructure, hardness and residual stress are the output parameters. The purpose is to vary all factors simultaneously over a set of planned experiments and then to analyze results to determine a mathematical model to interpret and predict results.

Machining was conducted on a RAMO RTN 20 Turning Center. The cutting tool used for the DoE was of Mitsubishi brand, reference SDJCL1616H11 with rhombic carbide inserts of grade HTi10 reference DCGT11T3 with nose radius 0.4 and 0.8 mm and a sharp cutting edge of 2μm. This tool is recommended to machine soft material and is called in the rest of this paper tool T1. Additional experiments were conducted with the tool T2 from SAFETY brand, reference SVJCL 1616 H13 with inserts VCGT 130304_PM5 585 Or 5000 (nose radius r_ε=0.4 mm and cutting edge of 31 μm). Both tools T1 and T2 have the same cutting and clearance angles. All machining tests were performed dry.

For the DoE, a fractional factorial plan was used with 2^{4-1} experiments. The number of runs was limited to the minimum number of experiments for a DoE with 4 factors, consequently high order interactions (square effect and 3 or more interaction factors) cannot be calculated but they have normally no interest. As the relationship between a factor and an output parameter can be curve linear, 2 center-point runs are added in the center of the DoE. In

total, the test design has 10 runs. The explored cutting conditions are presented in Table 2. Due to confidential issues, cutting parameters are expressed as a percentage of cutting conditions V_c*, a_p* and f* given by Mitsubishi for this tool in machining aluminum alloys. There are 3 factors at 3 levels and one factor at 2 levels. Preliminary tests and machine capacity enabled to delimit the level of the factors. The matrix design is presented in Table 3 where -1 denotes low level, 0 medium level and 1 high level. Cutting conditions for additional machined tests performed with the tool T2 can be seen in the Table 4 and are also expressed as a percentage of V_c*, a_p* and f*. Literature review (Tonshoff and Winkler 1997) and preliminary tests have shown that tool wear can be neglected if the turn travel is under 300 m, consequently one insert for each tool was used for all the machining tests. The response surface methodology was processed using the JMP 6.0.2 Software.

Table 2. Variation range of cutting conditions

Cutting speed, V_c	From 27% to 107% of V_c*
Depth of cut, a_p	From 33% to 100% of a_p*
Feed, f	From 25% to 150% of f*
Nose radius, r_ε	0.4 - 0.8

Table 3. Design matrix with tool T1

Run N°	V_c	a_p	f	r_ε
1	-1	-1	1	1
2	-1	1	1	-1
3	1	-1	-1	1
4	-1	1	-1	1
5	0	0	0	-1
6	-1	-1	-1	-1
7	1	1	1	1
8	0	0	0	1
9	1	-1	1	-1
10	1	1	-1	-1

Table 4. Additional tests with tool T2

Run N°	V_c (% of V_c*)	a_p (% of a_p*)	f (% of f*)
11	16%	67%	25%
12	32%	67%	25%
13	8%	133%	75%
14	8%	67%	75%

2.2. Characterization of surface integrity

Surface roughness was measured with a Marh PKG 120 profilometer according to DIN EN ISO 4288 (1998). Machined surfaces were observed using a Scanning Electron Microscope. For microstructural characterisation, metallurgical samples were cut and cold mounted. After mechanical polishing, a 3% Nital etching solution was used to reveal grain structures. Observations were made with optical microscopy. Microhardness measurements below the machined surface were performed using Mitutoyo brand MVK-H1 type equipment with a Vickers indenter and a load of 10 g during 20 s. Each plotted point at a given depth was averaged over 5 measurements. Residual stresses were obtained by X-ray diffraction using the $\sin^2 \psi$ method. The Set-X brand goniometer was used to perform residual stresses on the surface along the feed direction. The total penetration depth of the X-Ray beam for Mg is 38 μm.

3. Results and discussion

3.1. Surface roughness

The highest surface roughness was obtained for the run n°2 (R_t = 33.81 µm), and the smoothest surface was induced by the run n°4 (R_t = 1.41 µm). Figure 1 shows factor effects on surface roughness. As expected, significant parameters are feed *f*, nose radius r_ε and feed and nose radius interaction $f.r_\varepsilon$. Roughness improves while the feed decreases and nose radius increases. The equation obtained for the model by regression with the 2 influential parameters and interaction is:

$$R_t = 8.56 + 88.33 \cdot f - 19.92 \cdot r_\varepsilon - 165.49\left(f - 0.146\right)\left(r_\varepsilon - 0.6\right) \quad (1)$$

Although the model catches influential parameters, it does not predict satisfactorily surface roughness in the range of explored machining conditions, since the experimental design was reduced to a minimum number of tests and cannot identify square effect such as f^2 and r_ε^2. However, experimental roughness values R_t can be fitted (Figure 2) by the following geometrical model:

$$R_t = 1000 \cdot \left(r_\varepsilon - \sqrt{r_\varepsilon^{\,2} - \frac{f^2}{4}} \right) \quad (2)$$

The geometrical model offers also good correlation with additional surface roughness performed with the tool T2 (Figure 2).

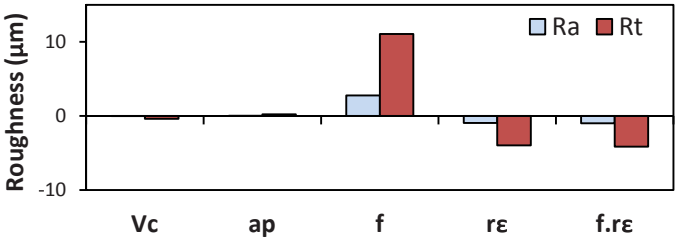

Fig. 1. Effects plotted for surface roughness obtained with the DoE

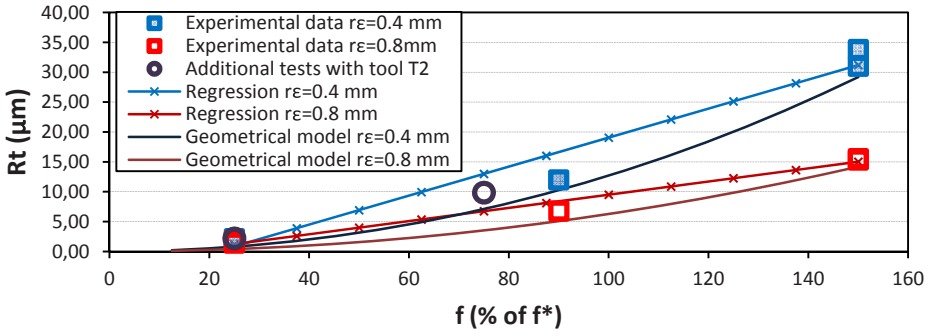

Fig. 2. Feed and nose radius effects on surface roughness

In this study, cutting speed has no influence on surface roughness R_a or R_t. However, SEM examination of machined surfaces revealed that surfaces produced by high feed and low speed (runs n°1 and 2) present tears and cracks mainly located close to Mg-Nd precipitates (Figure 3-a). While the cutting speed increases, chip becomes

more continuous and surface defects disappear (Figure 3-b). For low feed, the cutting speed seems to have no significant influence on machined surface.

All surfaces performed with the tool T2 present cracks and tears, which gives the impression of an orange peel with naked eyes (Figure 3-c-d). These surfaces defects are probably due to the round edge radius (31 μm instead of 2 μm for tool T1) and the coating (no polished insert instead of tool T1) of the insert which increase plowing effects and rubbing between tool and workpiece and generate poor surface quality. The beneficial effect of cutting speed to improve surface quality while increasing V_c is also noted for the Tool T2. However, even at high speed (run n°12) surface defects (tears) remain visible. Decreasing feed lead to improve surface quality since the size of the uncut chip thickness is reduced (Figure 3-c). No influence of depth of cut on surface roughness has been noticed for both tools.

Thus, to obtain optimal surface roughness (surface without defects) in turning, high cutting speeds must be privileged with a sharp tool, particularly for feed higher than 75%.f*.

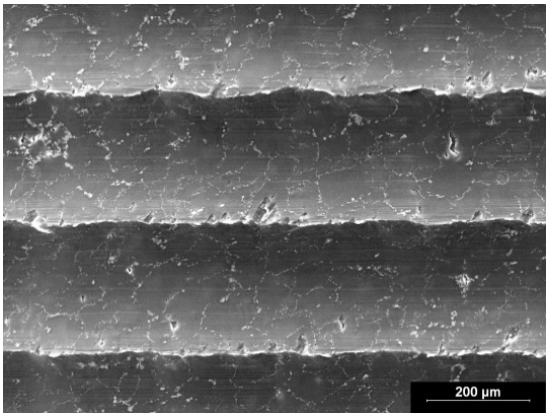

(a) Run n°2: Vc = 27%.Vc*, ap = 100%.ap*, f=150%.f* and rε = 0.4 mm, Tool T1

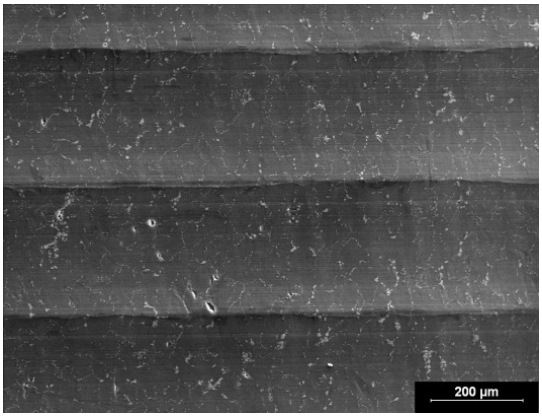

(b) Run n°7: Vc = 107%.Vc*, ap = 100%.ap*, f=150%.f* and rε = 0.4 mm, Tool T1

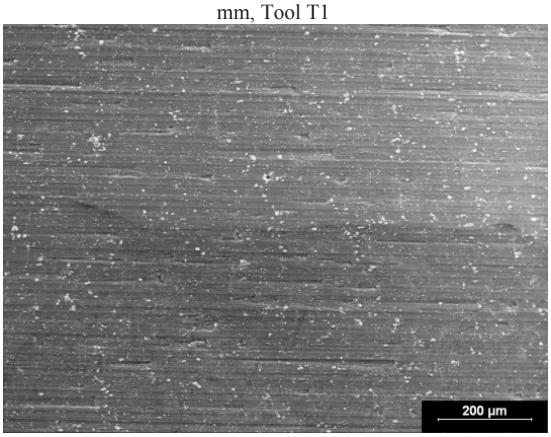

(c) Run n°11: Vc = 16%.Vc*, ap = 67%.ap*, f=25%.f*, Tool T2

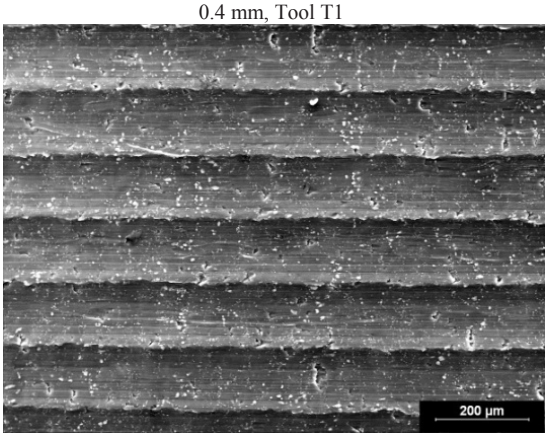

(d) Run n°13: Vc = 8%.Vc*, ap = 133%.ap*, f=75%.f*, Tool T2

Fig. 3. Machined surface for different cutting conditions

3.2. Microstructure

The Figure 4 shows microstructures below the machined surface for different cutting conditions. For all cutting conditions performed with the tool T1, grains are cut at the machined surface, and are usually twinned. Depth under machined surface affected by deformation twins increases with the depth of cut a_p. High feed f contributes to generate twinning at greater depth even if the depth of cut a_p is low. Thus, for machining conditions with low feed and depth of cut (runs n°3 and 6), few twinned grains are observed and depth under machined surface affected by

twinning is about 50 µm (Figure 4-b). Depth with plastic deformation twins is about 100 µm for tests with low depth of cut and high feed (runs n° 1 et 9) (Figure 4-a). Finally, for severe cutting conditions where $a_p = 100\%.a_p^*$, twins are present from the machined surface up to 200 µm depth (Figure 4-c and d). Thus, twinning predominates to accommodate deformation during machining of the wrought Elektron21, and deformation twins becomes larger with the increase of cutting forces corresponding to high feed or high depth of cut. Similar twinned microstructures were obtained during the dry turning of AZ31B (Pu et al 2012). Magnesium alloys have a hexagonal closed pack structure (hcp) where slip systems are limited. Although widely spread values of critical resolved shear stresses (CRSS) in the different slip and twinning systems have been reported, they are generally ordered: $CRSS_{basal} < CRSS_{twinning} < CRSS_{primatic} \leq CRSS_{pyramidal}$ (Agnew et al 2001, Agnew et al , Agnew et al 2005). Even at high temperatures, twinning is a major mode of deformation, since the CRSS of twinning is temperature independent in magnesium alloys (Barnett 2003, Ulacia et al 2010). No dynamic recrystallization was noticed for the different cutting conditions, in contrast to what could be observed in the machining of AZ31 (Pu et al 2012) Temperatures induced by cutting conditions are probably under 150°C (temperature obtained for more severe machining conditions in the turning of AZ31 (Pu et al 2012)) whereas dynamic recrystallization appears for temperatures higher than 200°C (Ulacia et al 2010, Samman and Gottstein 2008, Galiyev 2001). In addition, deformation rates during machining are very high, whereas diffusion mechanism processes which enable dynamic recrystallization are slow (Ishikawa et al 2005, Watanabe et al 2007).

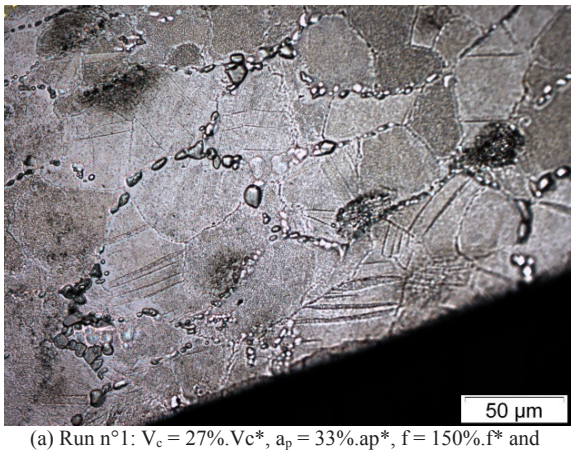

(a) Run n°1: $V_c = 27\%.Vc^*$, $a_p = 33\%.ap^*$, $f = 150\%.f^*$ and $r_\varepsilon = 0.4$ mm

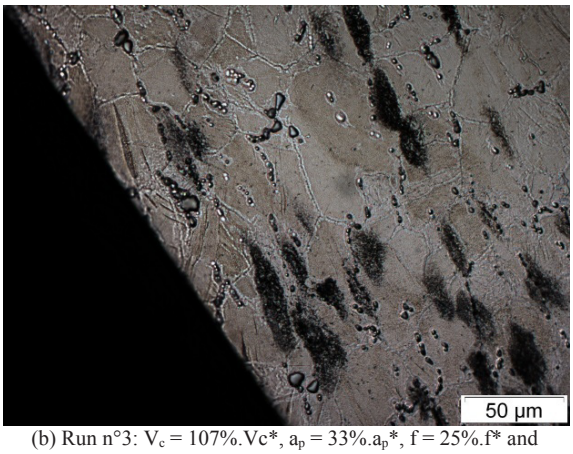

(b) Run n°3: $V_c = 107\%.Vc^*$, $a_p = 33\%.a_p^*$, $f = 25\%.f^*$ and $r_\varepsilon = 0.8$mm

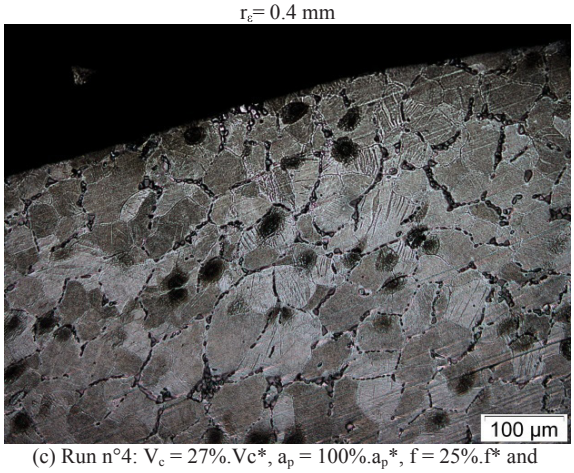

(c) Run n°4: $V_c = 27\%.Vc^*$, $a_p = 100\%.a_p^*$, $f = 25\%.f^*$ and $r_\varepsilon = 0.8$mm

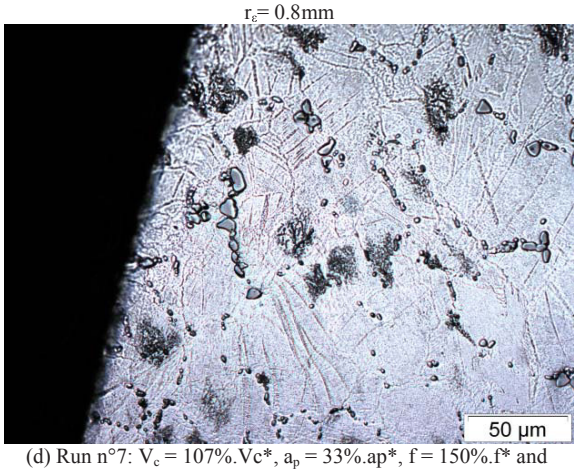

(d) Run n°7: $V_c = 107\%.Vc^*$, $a_p = 33\%.ap^*$, $f = 150\%.f^*$ and $r_\varepsilon = 0.8$mm

Fig. 4. Microstructures below machined surface for different cutting conditions

Twinning has a detrimental effect on fatigue life in magnesium alloy since fatigue cracks easily initiate and propagate along deformation twins (Nascimento et al 2010, Koike et al 2010). As a consequence, cutting conditions should be restricted to low feed and depth of cut to avoid high depth under machined surface with plastic deformation twins. No influence of cutting speed and nose radius have been noticed, the choice can be made in relation with chip flow and other surface integrity parameters.

3.3. Residual stress

Figure 5 presents the residual stresses in axial direction obtained for the tool T1 and the tool T2. Residual stresses performed with the tool T1 with the sharp edge radius are low and in tension (mainly under 50MPa) whereas the tool T2 with the round edge radius causes higher residual stresses in compression (mainly between -50MPa to -100MPa). Generation of tensile/compressive residual stresses is a competition between mechanical effects induced by cutting forces and thermal effects produced by friction at tool chip and tool workpiece interfaces. Increasing cutting edge radius from 2 μm to 31 μm generates an increase of uncut chip thickness and therefore cutting forces, leading to higher level of work hardening into subsurface. Similar observations were made in milling and turning of MgCa0.8 magnesium alloy while increasing edge radius (Denkena et al 2011). An opposite trend was obtained by Pu et al (2012). While increasing edge radius, higher temperatures were observed at tool tip, reducing the peak compressive residual stress. However, these high temperatures are due to higher feed and cutting speed than in the present study, which induced more friction at tool tip.

Analysis of the DoE enables to highlight the influence of feed and depth of cut on residual stresses. An augmentation of feed leads to increase residual stresses in tension, while increasing depth of cut means to reduce residual stresses. The obtained results suggest that when the feed increases, friction at tool interface increases and thus thermal effects become predominant compared to mechanical effects and generate high tensile residual stresses. On the contrary, when depth of cut increases plowing effect increases and thermal effects are balanced by mechanical effects leading to low tensile stresses. No influence has been noticed for nose radius and feed on residual stress. However the correlation parameter between experimental and model values R^2 is low (R^2=0.71). This means that the experimental design cannot catch satisfactorily influential machining parameters on residual stresses and that further experiments should be conducted.

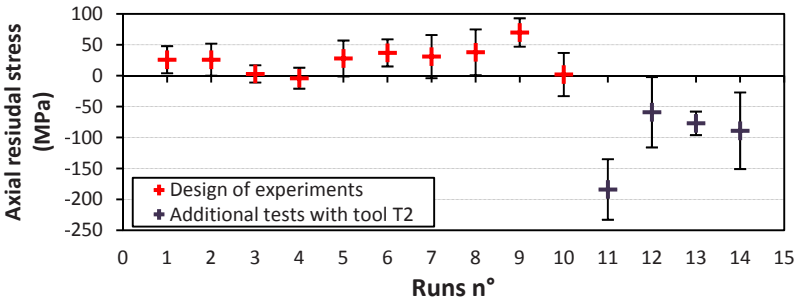

Fig. 5. Residual stresses along feed direction for different cutting conditions

Compressive residual stress is known to be beneficial for fatigue life, since it promotes crack closure and retards crack initiation via reducing the driving force at the crack tip. However, this beneficial effect can be reduced, when roughness is high with a lot of surface defects. In magnesium alloy, improvement of fatigue strength by shot peening have been shown with high or medium level of compressive residual despite surface defects and high roughness (Zhang et al 2010, Liu 2013). Thus, the tool T2 with the round edge radius presents interesting possibility to improve fatigue life with compressive residual stresses generated while machining. The run n°11 with intermediate cutting speed, low feed and intermediate depth of cut offer a good compromise between high compressive residual stresses and little surface defects.

3.4. Hardness

The hardness variation with depth under the machined surface is shown in Figure 6. A high dispersion of hardness measurements represented by error bar was observed (Figure 6-a). Even though each plotted point is an average of several values, hardness curves oscillates around the mean core hardness value, making difficult to interpret the results according to the different cutting conditions. To minimize dispersion of hardness values, a preliminary study was conducted to choose the best indenter load (i.e imprint size). Even increasing the size of imprint, the dispersion was not reduced drastically, thus the smallest size of imprint was chosen to measure hardness as close as possible from machined surface. The chosen diagonal length of the imprint size is about 17 µm while average grain sizes is 5 µm, consequently hardness is average on several grain. The dispersion of results can be explained by the presence of globular precipitates of Nd and fine precipitation rich in Zn-Zr which are harder than the α-matrix. Thus, the micro hardness methodology set up in this study is not suited to this alloy, due to the presence of several phases. This observation was already made in a two phase titanium alloy (Moussaoui et al 2012).

Nevertheless, surfaces performed at low cutting speed (Runs n°11, 13 and 14 where $V_c < 67\%.V_c$*) with the tool T2 (Figure 6-b) present hardening just below the machined surface, whereas softening is noticed for surfaces machined with the tool T1 (Figure 6-a) and with the tool T2 at high cutting speed (Run n°12). The hardening phenomenon obtained with the tool T2 is probably due to round edge radius of inserts which increases mechanical deformation. These results are in correlation with residual stress measurements. For the run n°12, high cutting speed leads to increase thermal effect which outweighs the mechanical deformation and work hardening.

High hardness in the surface layer increases its yield stress and thus fatigue life (Sasahara 2005). As a consequence, a tool with round edge radius must be privileged with low or medium cutting speed to improve fatigue strength.

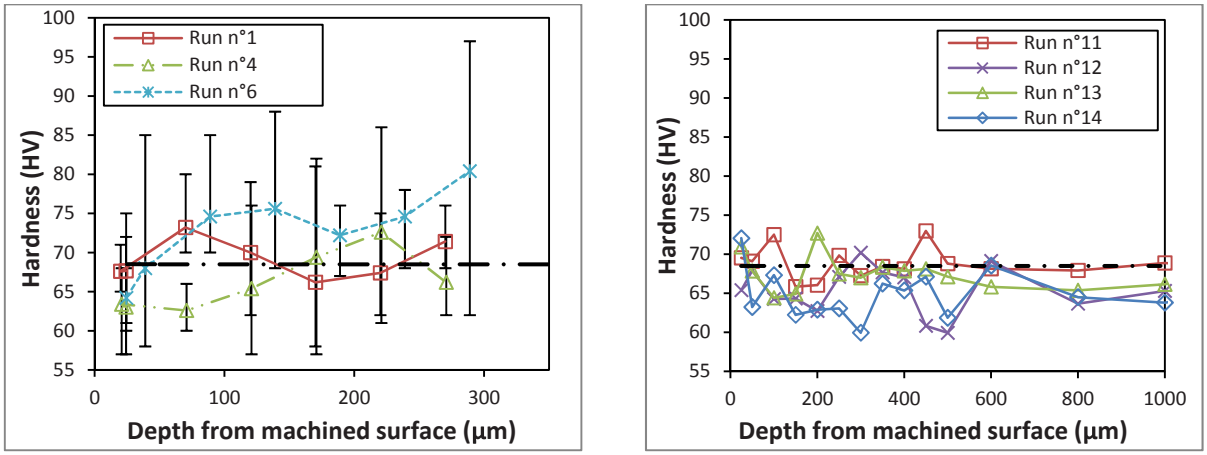

Fig. 6. Microhardness variation with depth under the machined surface

4. Conclusions

In this study, effect of machining parameters on surface integrity of the forged Elektron21 was investigated through a design of experiment. This study has demonstrated that feed, nose radius and nose feed interaction have significant effects on surface roughness, therefore a classical geometrical model offers good prediction of surface roughness for the tested cutting conditions. Deformation under machined surface is accommodated by twinning and increasing feed or depth of cut leads to generate twinning deformation at higher depth. With a sharp tool, tensile residual and softening in the surface layer are performed, whereas with a round edge radius compressive residual stress and hardening can be achieved if cutting speed is low or medium. Thus, the study suggests that to

improve fatigue strength, round edge radius must be privileged with low or medium cutting speed and low feed to limit surface defects. Selected cutting conditions should be reproduced on fatigue specimen, which will be tested in the future to confirm the expectation.

Acknowledgements

The authors would like to thank the CARAIBE project, which is supported by national funds (FUI) and the AEROSPACE VALLEY cluster.

References

Advesian M. M., Baker H. (Eds). Magnesium and Magnesium alloys. ASTM International Materials Park (2000).

Agnew R., Tom C.N., Brown D.W., Holden T.M., and Vogel S.C.. Application of texture simulation to understanding mechanical behavior of Mg and solid solution alloys containing Li or Y. Acta Materialia, 49: 4277–4289, 2001.

Agnew S. R. and Duygulu O.. Plastic anisotropy and the role of non-basal slip in magnesium alloy AZ31B. International Journal of Plasticity, 21 :1161-1193, 2005.

Agnew S.R., Tom C.N., Brown D.W., Holden T.M., and Vogel S.C.. Study of slip mechanisms in a magnesium alloy by neutron diffraction and modeling. Scripta Materialia, 48: 1003-1008, 2003.

Al-Samman T. and Gottstein G.. Dynamic recrystallization during high temperature de- formation of magnesium. Materials Science and Engineering, 490: 411–420, 2008.

Barnett M. R.. A taylor model based description of the proof stress of magnesium AZ31 during hot working. Metallurgical and materials transactions, 34 A: 1799–1806, 2003.

Bhowmick S., Lukitsch M. J., and Alpas A. T.. Dry and minimum quantity lubrication drilling of cast magnesium alloy (AM60). Int. J. of Machine Tools & Manufacture, 50: 444–447, 2010.

Bhuiyan M. S., Mutoh Y., McEvily A.J.. The influence of mechanical surface treatments on fatigue behavior of extruded AZ61 magnesium alloy. Materials Science and Engineering: A, 549 (2012), pp. 69-75.

Denkena B., Lucas A., Thorey F., Waizy H., Angrisani N., and Meyer-Lindenberg A.. Special Issues on Magnesium Alloys, chapter 5 - Biocompatible Magnesium Alloys as Degradable Implant Materials - Machining Induced Surface and Subsurface Properties and Implant Performance. 2011.

Fang F. Z., Lee L. C., and Liu X. D.. Mean flank temperature measurement in high speed dry cutting of magnesium alloy. Journal of Material Processing Technology, 167: 119–123, 2005.

Galiyev A., Kaibyshev R., and Gottstein G.. Correlation of plastic deformation and dynamic recrystallization in magnesium alloy ZK60. Acta Materialia, 49: 1199–1207, 2001.

Gariboldi E.. Drilling a magnesium alloy using pvd coated twist drills. Journal of Materials Processing Technologies, 134 :287–295, 2003.

Ishikawa K., Watanabe H., and Mukai T.. High strain rate deformation behavior of an AZ91 magnesium alloy at elevated temperatures. Materials Letters, 59: 1511-1515, 2005.

Koike J., Fujiyama N., Ando D., and Sutou Y.. Roles of deformation twinning and dis- location slip in the fatigue failure mechanism of AZ31 Mg alloys. Scripta Materialia, 63: 747-750, 2010.

Liu W., Wu G., Zhai C., Ding W., and Korsunsky A. M.. Grain refinement and fatigue strengthening mechanisms in as-extruded Mg–6Zn–0.5Zr and Mg–10Gd–3Y–0.5Zr magnesium alloys by shot peening. International Journal of Plasticity, 2013. Accepted Manuscript.

Moussaoui K., Mousseigne M., Senatore J., Chieragatti R., Monies F.. Influence of milling on surface integrity of Ti6Al4V—study of the metallurgical characteristics: microstructure and microhardness. Int. J. of Advanced Manufacturing Technology, 63, 2012

Nascimento L., Yi S., Bohlen J., Fuskova L., Letzig D., and Kainer K. U.. High cycle fatigue behaviour of magnesium alloys. Procedia Engineering, 2: 743–750, 2010.

Pu Z., Outeiro J.C., Batista A.C., Dillon Jr O.W., Puleo D.A., and Jawahir I.S.. Enhanced surface integrity of AZ31B mg alloy by cryogenic machining towards improved functional performance of machined components. International Journal of Machine Tools & Manu- facture, 56: 17–27, 2012.

Sasahara H. The effect on fatigue life of residual stress and surface hardness resulting from different cutting conditions of 0.45%C steel, Int. J. Machine Tools and Manufacture, Vol. 45, 2005, pp.131–136.

Tonshoff H. K. and Winkler J.. The influence of tool coatings in machining of magnesium. Surface and Coatings Technology, 94-95 :610–616, 1997.

Ulacia I., Dudamell N.V., Galvez F., Yi S., Perez-Prado M.T., and Hurtado I.. Mechanical behavior and microstructural evolution of a Mg AZ31 sheet at dynamic strain rates. Acta Materialia, 58 :2988–2998, 2010.

Watanabe H., Ishikawa K., and Mukai T.. High strain rate deformation behavior of Mg- Al-Zn alloys at elevated temperatures. Key Engineering Materials, 340-341: 107–112, 2007.

Zhang P., Lindemann J., Leyens C.. Influence of shot peening on notched fatigue strength of the high-strength wrought magnesium alloy AZ80. Journal of Alloys and Compounds, 497 (2010), pp. 380-385.